Continuous-wave electron spin resonance studies of porphyrin and porphyrin-quinone triplet states

Burkhard Kirste,* Peizhu Tian, Werner Kalisch and Harry Kurreck *
Institut für Organische Chemie, Freie Universität Berlin, Takustrasse 3, D-14195 Berlin, Germany

CW ESR studies of the photoexcited triplet states of a series of porphyrins and covalently linked porphyrin-quinones have been performed in isotropic and anisotropic (liquid-crystalline) frozen solutions. In frozen nematic solutions, the appearance of the spectra is strongly dependent on the orientation of the sample relative to the external magnetic field. This fact allows a differentiation between the z and x,y axes and hence a more accurate determination of the zero-field splitting parameters D and E. Spectrum simulation and fitting aided in the interpretation of the experimental results and the extraction of the relevant parameters. In the case of some porphyrin-quinones, steady-state triplet ESR signals cannot be observed, which is ascribed to singlet-electron transfer enhanced by folding of the quinone acceptor over the porphyrin donor. The doublet signal of porphyrin or chlorin cation radicals, which is also observed, appears in emission under certain conditions, indicative of the radical triplet pair mechanism.

Introduction

The primary electron-transfer process in native photosynthetic reaction centres is known to proceed *via* the singlet excited state of the *special pair* in the temperature range from room temperature down to ~5 K, but formation of the triplet state can be enforced by blocking the electron transfer by pre-reduction of the quinone Q_A.[1] Knowledge of the properties of the triplet excited states of porphyrins is important, because light-induced electron transfer between porphyrin donors and quinone acceptors, *e.g.*, in biomimetic model compounds for photosynthetic reaction centres, may proceed *via* the triplet state provided that the viscosity of the solvent is suitably chosen.[2,3] The zero-field splitting parameters, notably the E parameter, depend on the electron distribution and differ in porphyrins and chlorins. In liquid-crystalline solutions, triplet ESR spectra provide a sensitive probe of the alignment of the molecules.[4–6] In covalently linked porphyrin-quinones, the distance between donor and acceptor affects the triplet lifetime.

Experimental

The syntheses of most of the porphyrins and porphyrin-quinones dealt with in this study have been published previously.[7,8] Sample concentrations were in the range between 0.5 mmol dm^{-3} and 1.5 mmol dm^{-3}; samples were degassed by flushing with argon for 30 min. The following solvents have been used: toluene, 30% 2-methyltetrahydrofuran (MTHF)–70% toluene (v/v), ethanol, liquid crystal 5CB (4-cyano-4'-pentylbiphenyl, nematic range 22.5–35.5 °C) and Triton X-100 reversed micelles (pH 7). ESR spectra were measured on a Bruker ER 200D-SRC ESR spectrometer, which was interfaced with a personal computer *via* a MetraByte DAS-16 board. The photoexcited states were generated by *in situ* irradiation through a slit in the ESR cavity with a 1000 W Hg–Xe lamp (Oriel) with a 570 nm cut-off filter (Schott) unless stated otherwise. Experimental conditions: microwave power 5 mW, field modulation 0.5 mT, gain 5×10^5, field sweep 90.08 mT.

Liquid-crystal samples were aligned by the following procedure. In a magnetic field of 0.8 T, samples were heated above the clearing point, and kept for 20 min in the isotropic phase; then the temperature was reduced at a rate of 4 K min^{-1} to the nematic phase and kept for 20 min at 300 K, then the samples were cooled at a rate of 4 K min^{-1} to 260 K and finally quickly to 110 K.

Results and discussion

In Fig. 1 (top), the high-field part of the ESR spectrum of compound **2** in the photoexcited triplet state in glassy toluene (110 K) is shown (solid line). An intense half-field signal ($\Delta m = 2$, $g = 4.03$) was also observed (at $B_{min} \approx 167.7$ mT, not shown). ESR spectra obtained in the aligned frozen nematic phase of the liquid crystal 5CB (at 110 K) are also depicted in Fig. 1, taken with the director L parallel to the static magnetic field B_0 (bottom) and with the director perpendicular to the magnetic field (centre). The determination of the zero-field splitting parameter D from the outermost turning points (B_{z1}, B_{z2}) is straightforward ($|D| = (B_{z2} - B_{z1})/2$), $|D| = (32.8 \pm 0.1)$ mT, $g_{zz} \approx 1.998$ (toluene, 110 K).

The situation regarding the x,y features is more complicated, because two distinct sets are observed: one set of x,y peaks gives rise to shoulders near the z peaks and near the strong doublet signal at the centre of the spectrum, the second set of 'averaged' x,y peaks appears halfway between the doublet signal and the z peaks. The distinction between x,y and z features is easier in the spectra taken in the aligned nematic phase. The liquid crystal 5CB has a positive anisotropy of the diamagnetic susceptibility ($\Delta\chi > 0$), hence the director L, *i.e.*, the long axes of the solvent molecules, are aligned parallel to the external field in the fluid nematic phase. Alignment of the 'flat' porphyrin molecules will obviously be with the in-plane (x,y) axes parallel to the director. Thus, the spectrum obtained in the frozen nematic phase with $L \| B_0$ will show mainly the x,y peaks, whereas the z peaks become predominant after rotation of the sample tube by 90° ($L \perp B_0$). Although the low-field z and y peaks (z_1,y_1) almost coincide, the respective high-field peaks (z_2,y_2) are easily distinguished in the aligned nematic phase ($g_{yy} > g_{zz}$).

For an accurate determination of the E parameter and as a check of our interpretation of the triplet ESR spectra, we have performed computer simulations using program POLFT described previously.[9] This program performs automated fitting to the experimental data starting with an initial guess of the zero-field splitting parameters (D, E) and the principal components of the g tensor. Convolution of the lineshape (Gaussian lineshape was assumed) was achieved by means of the Fourier transform technique. As a disadvantage, angular dependences of linewidths cannot be taken into account. Program POLFT was modified to take account of ordering in the nematic phase by multiplication of the calculated signal

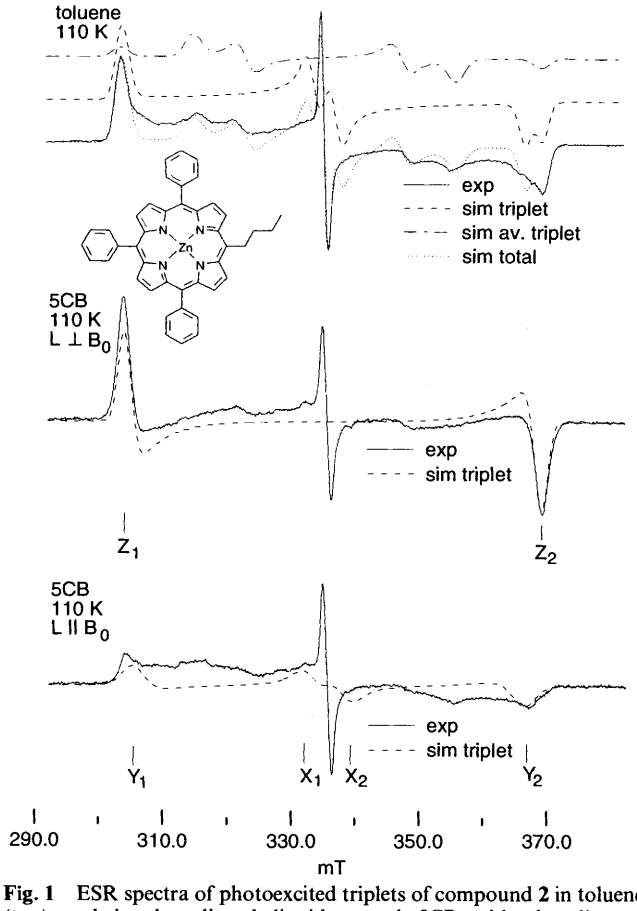

Fig. 1 ESR spectra of photoexcited triplets of compound **2** in toluene (top) and in the aligned liquid crystal 5CB with the director perpendicular (centre) and parallel (bottom) to the static magnetic field. Computer simulations are represented by dashed or dotted lines. Note that the splitting of the high-field *y*,*z* peaks, which can be seen in the liquid-crystalline solvent, is not resolved in the experimental spectrum taken in toluene.

intensities with the distribution function $f(\theta)$,[10,11] as shown in eqns. (1) and (2).

$$f(\theta) = \exp(a \cos^2 \theta) \qquad (L \| B_0) \qquad (1)$$

$$f_{perp}(\theta) = \exp(a \sin^2 \theta) \qquad (L \perp B_0) \qquad (2)$$

In the case of non-axially symmetric molecules, there may be effects due to preferential in-plane alignment, *e.g.* as that shown in eqn. (3).

$$f_{perp}(\theta,\varphi) = \exp(a \sin^2 \theta \sin^2 \varphi) \qquad (L \perp B_0) \qquad (3)$$

The parameter a is related to the order parameter $\bar{P}_2$ (also denoted as O_{33}) by eqn. (4).

$$\bar{P}_2 = \frac{\int_0^{\pi} \frac{1}{2}(3 \cos^2 \theta - 1) \exp(a \cos^2 \theta) \sin \theta \, d\theta}{\int_0^{\pi} \exp(a \cos^2 \theta) \sin \theta \, d\theta} \qquad (4)$$

Before starting the fitting procedure, baseline correction of the experimental spectra was performed and the strong doublet signal in the centre was subtracted. In the simulations referring to the nematic phase, a high degree of ordering was assumed ($a = -10$ corresponding to $\bar{P}_2 = -0.425$), see the dashed lines in Fig. 1. The alignment exhibited by the experimental spectra is less perfect, either because of a lower overall degree of ordering or because of the multidomain structure of the samples. Using the zero-field splitting parameters obtained by fitting the spectra taken in the nematic phase ($D = 32.3$ mT, $E = 9.5$ mT, $g_{xx} \approx 2.004$, $g_{yy} \approx 2.003$, $g_{zz} \approx 1.998$) as a starting point, the spectrum taken in toluene was analysed in more detail. Thus, by a combination of spectrum fitting and subtraction, a differentiation between the two triplet species with large and small E values was possible, see Fig. 1 (top): $D = 32.9$ mT, $E = 9.9$ mT, $E_{av} = 2.8$ mT.

The position of the half-field signal B_{min} ($\Delta_m = 2$) is given by eqn. (5)[12] where eqn. (6) holds.

$$g\mu_B B_{min}/h\nu = \{\tfrac{1}{4} - \tfrac{1}{3}(D^*/h\nu)^2\}^{\frac{1}{2}} \qquad (5)$$

$$D^* = \{D^2 + 3E^2\}^{\frac{1}{2}} \qquad (6)$$

The experimental value of $D^* = 32.4$ mT suggests $E \approx 0$; it is not compatible with the larger E-value.

Similar results were obtained for a series of other zinc porphyrins, see Table 1: D values are in the range 31.7–33.0 mT, E-values are $E = 9.5$–10.1 mT, and the largest variation is found for the 'averaged' E parameter, $E_{av} = 0$–2.8 mT.

In Fig. 2, the corresponding results for the photoexcited triplet of the chlorin ZnTPC **4** are depicted, namely the experimental ESR spectra taken in toluene and in the liquid crystal 5CB along with computer-simulated spectra. In this case only the 'averaged' triplet spectrum is observed, and the *x*,*y* peaks are much broader than the *z* peaks. (In the simulations, angular-independent linewidths are assumed.) D- and E_{av}-values are somewhat larger than those of the porphyrins: $D = 34.3$ mT, $E_{av} = 3.2$ mT (toluene, 120 K); $D = 33.9$ mT, $E_{av} = 4.3$ mT (5CB, 110 K).

In 5CB, the doublet signal in the spectrum centre shows a well resolved quintet pattern due to hyperfine interaction with four equivalent protons. For both orientations ($L \| B_0$ and $L \perp B_0$) the same hyperfine splitting constant of 0.647 mT is measured (value from spectrum fitting), hence the hyperfine anisotropy must be small. Similar observations have been made previously,[13] and the spectrum has been assigned to the ZnTPC radical cation with hyperfine splitting due to four equivalent protons in the dihydropyrrole ring. The same species can be generated chemically by oxidation with iodine.

In Fig. 3, the ESR spectra of the photoexcited triplets of two covalently linked porphyrin-quinones are compared with those of the respective hydroquinones. In the case of compound **7** (Fig. 3, top), the spectrum of the quinone is essentially identical with that of the hydroquinone, except for the reduced signal intensities. In the second case, the crown ether compound **10**, no signal due to the porphyrin-quinone has been observed. This behaviour of crown compound **10** has already been reported in a previous paper[3] and ascribed to fast singlet-electron transfer caused by a diminished porphyrin-quinone distance due to folding of the quinone acceptor over the porphyrin donor. In analogy to these examples, triplet ESR spectra of several porphyrin-quinones with rigid spacers (*cis*- or *trans*-1,4-cyclohexylene bridges) have been observed, but not from those with flexible 1,4-butylene (tetramethylene) links.

In Fig. 4, the ESR spectra of the photoexcited triplets of compounds **13** (top) and **14** (bottom), two covalently linked porphyrin-quinones bearing three perfluorophenyl rings at the porphyrin ring, taken in the liquid crystal 5CB, are shown. The spectrum of compound **13** taken in toluene (not shown) reveals a well resolved triplet powder pattern with considerable rhombic splitting ($D = 34.9$ mT, $E = 3.8$ mT, $g_{xx} \approx 2.005$, $g_{yy} \approx 2.004$, $g_{zz} \approx 1.998$). In the aligned nematic phase, essentially either the *y* peaks (director $L \| B_0$) or the *x* and *z* peaks (director $L \perp B_0$) are observed, *i.e.*, there is a pronounced preference for alignment along the *y* axis. In the simulations, the *y* axis was taken as the crucial axis, and an a parameter of 3.5

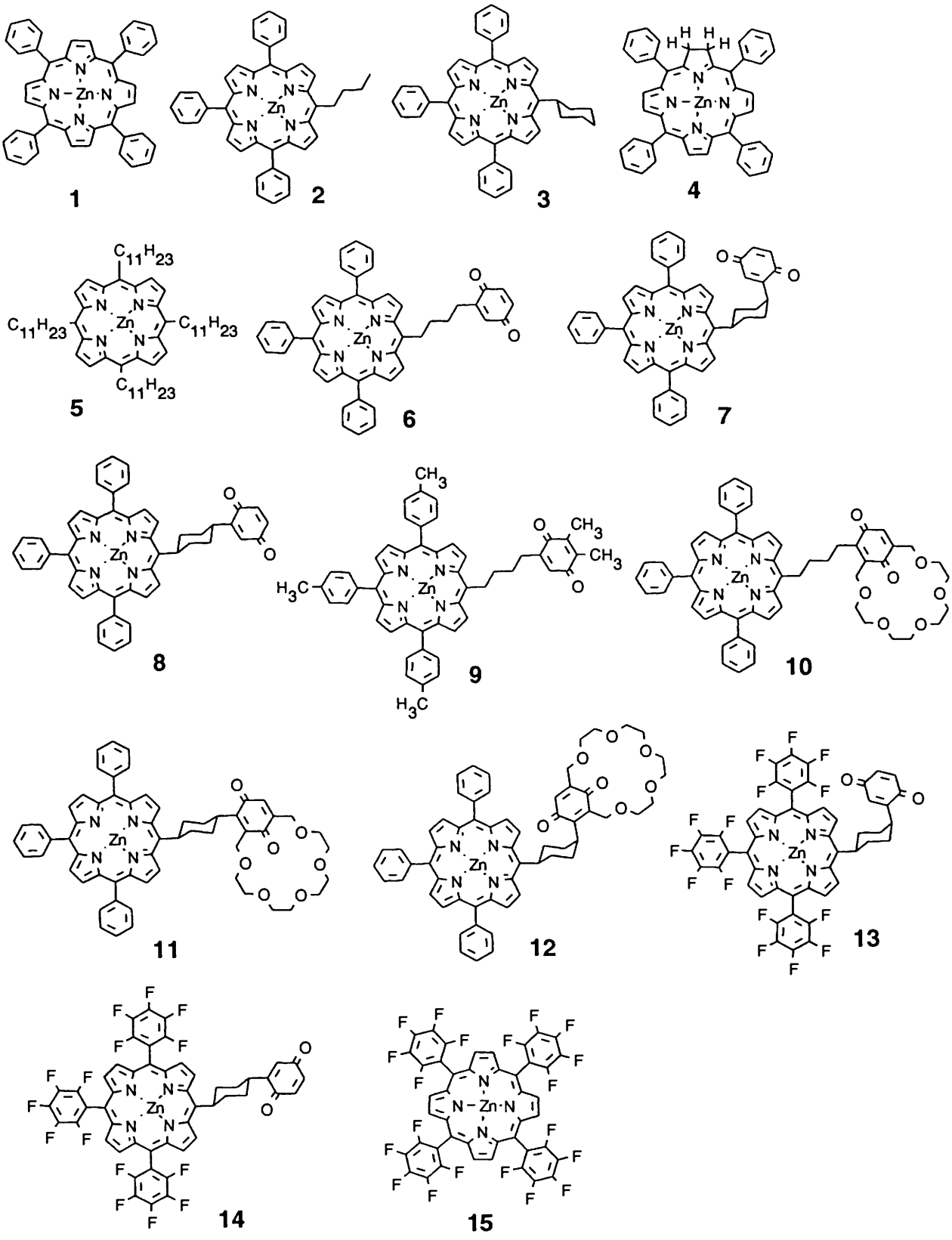

corresponding to $O_{yy} = \bar{P}_2 = 0.5$ was used. Just the opposite behaviour is observed for compound **14**: here the x peaks dominate the spectrum when $L \| B_0$, and the y and z peaks when $L \perp B_0$.

In nematic phases, alignment of solute molecules is usually along the longest molecular axis. From molecular models, dimensions (including van der Waals radii) are estimated as follows; F–F (axis passing through the two pentafluorophenyl rings): 2.11 nm, F–H (axis passing through pentafluorophenyl and cyclohexylene ring): 2.04 nm (**13**) and 2.48 nm (**14**), respectively. The directions of the 'long' molecular axes are indicated by dashed arrows in the formulae depicted in Fig. 4. It seems reasonable to assume that the position of the quinone moiety, *i.e.* axial (**13**) or equatorial (**14**), does not have a significant influence on the spin-density distribution within the porphyrin moiety and hence the zero-field splitting parameters. (This assumption has been confirmed by calculations, *vide infra*.) Thus, we attribute the different behaviour of the two

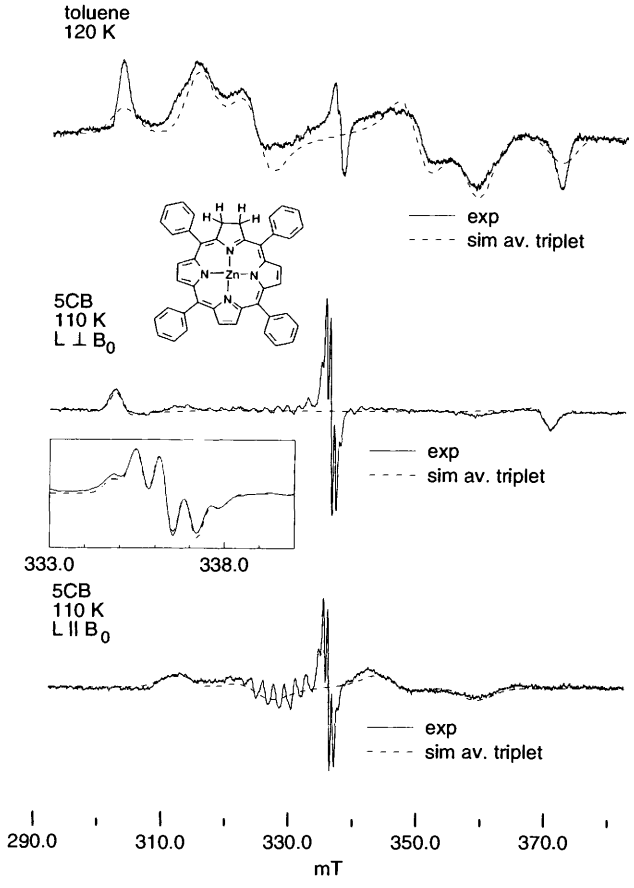

Fig. 2 ESR spectra of photoexcited triplets of compound **4** (ZnTPC) in toluene (top) and in the aligned liquid crystal 5CB with the director perpendicular (centre) and parallel (bottom) to the static magnetic field. (The 'wavy' ESR signal around 330 mT stems from an impurity in the starting material.) Computer simulations are represented by dashed lines. The inset shows the signal of the ZnTPC radical cation on an expanded scale along with a computer simulation.

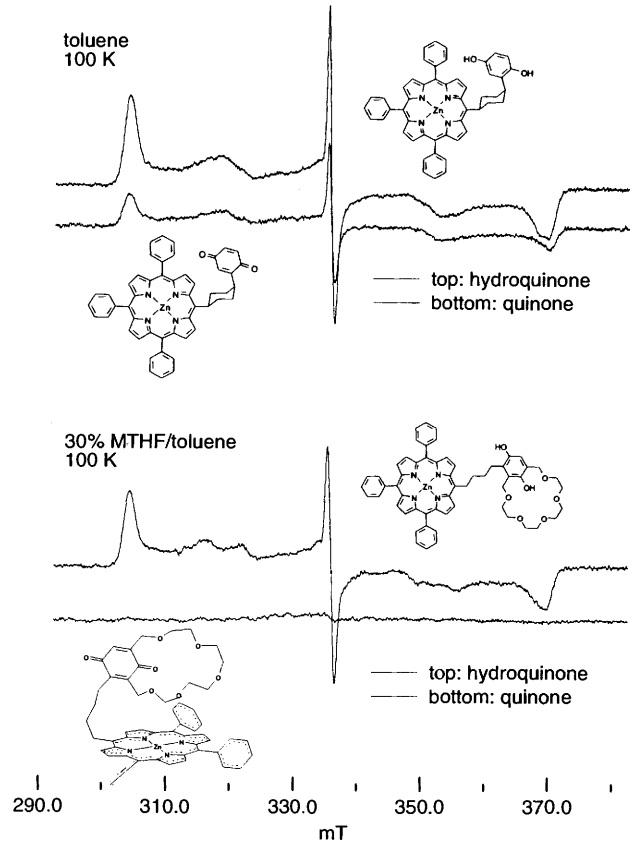

Fig. 3 Comparison of the ESR spectra of photoexcited triplets of two different porphyrin-quinones with those of the respective hydroquinones: **7** (top half) and **10** (bottom half)

molecules to a difference in preferential alignment, *i.e.*, along the axes indicated: the *x* axis being assigned to the axis through the cyclohexylene ring and the *y* axis to the axis through the two pentafluorophenyl rings. It has to be mentioned that the assumption of alignment along an axis passing through the *meso* positions would contradict a model used for the interpretation of time-resolved ESR spectra of the structurally similar compounds **7** and **8**.[2] Since rhombic splitting was not observed for the photoexcited triplets of other porphyrin quinones (**7**, **8**, **11**, **12**), *i.e.*, $E_{av} \approx 0$, information about their in-plane alignment is not accessible from the present study.

Fig. 5 depicts a series of ESR spectra from an experiment performed on ZnTPC **4** in fluid solution. First, ZnTPC radical cations were generated by irradiating a frozen solution in ethanol (1 min at 110 K) with light cut-off at 395 nm. After warming up to 190 K, the ESR spectrum of the ZnTPC radical cation is observed in absorption (hyperfine couplings 0.61 mT, 4 H, linewidth 0.64 mT). During irradiation, a second signal is building up which appears in emission. This emissive signal is a singlet with Gaussian lineshape and a peak-to-peak width of 0.82 mT; it is slightly shifted towards lower fields ($\Delta g \approx 0.0003$). We suggest that it arises from the radical triplet pair mechanism, *i.e.*, interaction of ZnTPC doublet radicals with ZnTPC triplets.[14] It should be mentioned that a *g* shift of the emissive signal has also been observed in ESR experiments on pre-reduced reaction centres of photosynthetic bacteria at 5 K.[15,16]

Discussion of the zero-field splitting parameters

The zero-field splitting of photoexcited porphyrin triplets and the anomalous ESR lineshapes have been discussed extensively in the literature.[17,18] Although the apparent D_{4h} (or D_4) symmetry of zinc porphyrins such as ZnTPP **1** should give rise to ESR spectra with axial symmetry ($E = 0$), the observation of a substantial rhombic contribution ($|E|$ almost $|D|/3$) is well established and attributed to Jahn–Teller splitting. Dynamic effects giving rise to a partial or complete averaging of the rhombic distortion may be due to various reasons, which will not be discussed here; they may be intra- or inter-molecular (dynamic Jahn–Teller effects, intramolecular discrete $\pi/2$ jumps, exciton interactions in aggregates), and ligation of solvent molecules with the central metal may have to be taken into account. In the porphyrins, porphyrin-quinones and porphyrin-hydroquinones studied here (except ZnTPP **1**, **5** and **15**), the D_{4h} symmetry is lifted by substitution, removing the degeneracy of LUMO and NLUMO (lowest and next lowest unoccupied molecular orbitals, respectively). In all cases except ZnTPC **4**, one of the *meso* positions is affected; the different symmetry of ZnTPC may be responsible for its slightly different behaviour.

The *D* parameters do not vary much (31.6–37.4 mT, see Table 1). In a very simple model for a delocalized planar triplet molecule, a value of 33 mT would correspond to two electrons moving on a circle with a diameter of 348 pm; the N–N distance is about 414 pm [$D = (3/4)g^2\mu^2_B/r^3$].[19] For a more detailed discussion of the *D* and *E* parameters, quantum mechanical calculations and **D**-tensor calculations are required. Frequently the following approximation (7) is used,[20,21] where *m*,*n*

$$D_{mn} = \tfrac{1}{2}g^2\mu_B^2 \sum_{i,j(i\neq j)} \rho_i\rho_j' \frac{r_{ij}^2\delta_{mn} - 3m_{ij}n_{ij}}{r_{ij}^5} \qquad (7)$$

denote the axes (*x*, *y*, *z*), *i*, *j* the atoms (p-orbitals), r_{ij} their

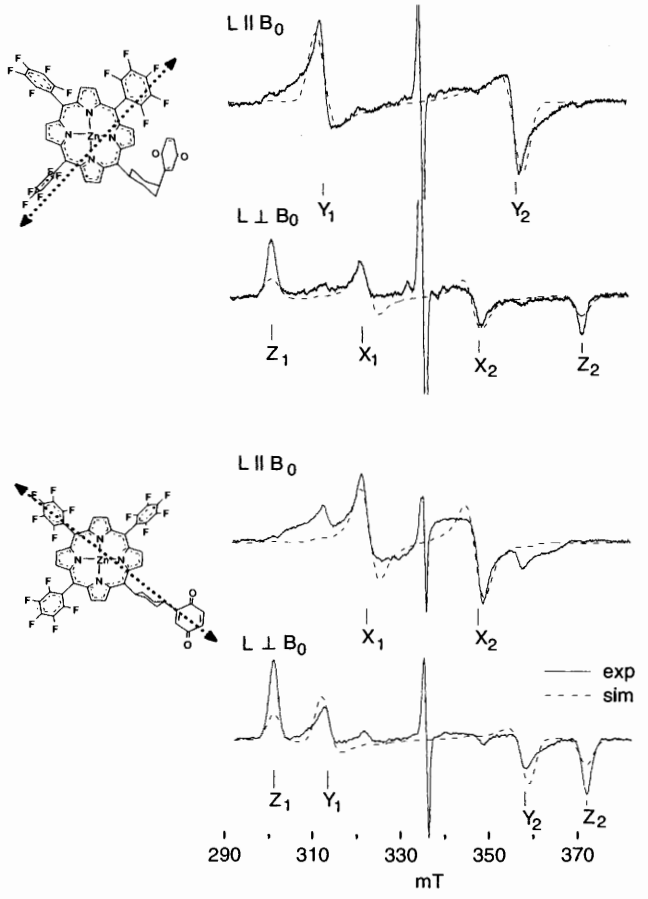

Fig. 4 ESR spectra of photoexcited triplets of fluoro compounds **13** (top) and **14** (bottom) in the aligned liquid crystal 5CB with the director parallel and perpendicular to the static magnetic field. Computer simulations are represented by dashed lines. The arrows in the formulas indicate the 'long' molecular axes.

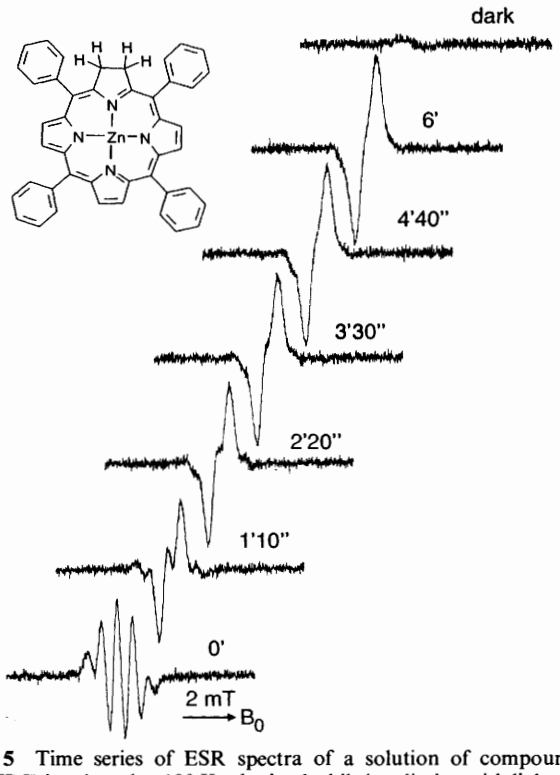

Fig. 5 Time series of ESR spectra of a solution of compound **4** (ZnTPC) in ethanol at 190 K, obtained while irradiating with light (cut-off at 395 nm). The numbers indicate the accumulated irradiation time at the beginning of each scan. The last trace (top) was recorded after turning off the light.

distances and ρ_i, ρ'_j the spin populations. After diagonalization of the **D**-tensor, D is three-halves the maximum component and E one-half of the difference of the other two components. Eqn. (7) is a reasonable approximation for biradicals with separated radical moieties but only a crude approximation for delocalized triplets such as porphyrins.[22] We have calculated π spin populations by the RHF/AM1 method (using Spartan 3.1.1 from Wavefunction Inc., SGI version) after optimizing the geometry by force-field calculations. The π spins were simply assumed to be located as point charges at the positions of the nuclei. As a check, we have obtained quite reasonable D- and E- values for the naphthalene triplet despite our simplifications.

For ZnTPP **1**, we have calculated $D = 54$ mT and $E = 0$ (average over the degenerate LUMO and NLUMO), for the fluorinated compound **15**, $D = 56$ mT and $E = 0$. In ZnTPC **4** and in the substituted compounds, the axial symmetry is lost. Consequently, the degeneracy of LUMO and NLUMO is lifted, and an unsymmetrical spin distribution is obtained. For ZnTPC **4**, we have calculated $D = 52$ mT and $E = 9.5$ mT; the energy splitting between LUMO and NLUMO is substantial ($\Delta E = 0.553$ eV, 1 eV = 96.485 kJ mol^{-1}). The fluorinated porphyrin-quinones **13** and **14** are of particular interest. For both compounds, $D = 57$ mT and $E = 5.0$ mT were obtained [$\Delta E = 0.180$ eV (**13**) and 0.172 eV (**14**)], and the absolute value of the zero-field splitting component in the y direction (axis through the two pentafluorophenyl rings) is in fact larger than that of the x component, in agreement with the assumptions made above (see Fig. 4). For the corresponding porphyrin-quinones without fluoro substituents, compounds **7** and **8**, the calculated values of $D = 55$ mT and $E = 3.9$ mT (LUMO) are not much different. However, the energy gap between LUMO and NLUMO is much smaller (0.041 and 0.035 eV); apparently, at the temperature of measurement (100 K) averaging essentially removes the rhombic splitting.

Conclusions

Photoexcited triplets of zinc porphyrins in isotropic and anisotropic glasses generally exhibit a superposition of ESR spectra due to triplet states with substantial rhombic distortion ($D \approx 32$ mT, $|E| \approx 10$ mT) and to dynamically averaged triplets (D unchanged, $|E| = 0$–3 mT). Dynamic averaging, which may occur intramolecularly over the two orbital components of the nearly degenerate triplet state or intermolecularly in the case of aggregation, is indicated by line broadening of the x,y components. Use of nematic glasses allows differentiation between the in-plane (x,y) zero-field splitting components (director parallel to the static external field) and the out-of-plane (z) component (director perpendicular to the field).

In covalently linked porphyrin-quinones, basically the same triplet ESR patterns are observed as in the constituent triplet porphyrins or the respective porphrin-hydroquinones. However, singlet-electron transfer from the porphyrin to the quinone reduces the signal intensities and may even prevent detection of the triplet spectrum. Thus, no triplet signal was observed in the case of a butylene (tetramethylene)-linked crown ether compound, which we ascribe to back folding. We conclude that continuous wave (CW) ESR experiments on photoexcited triplets of porphyrin-quinones can therefore supply important (qualitative) information about the electron-transfer properties.

Although in the porphyrin-quinones the four-fold symmetry of the porphyrin moiety is lifted, this fact was not borne out by the ESR spectra in most cases. Only compounds **13** and **14** were

Table 1 Zero-field splitting parameters of photoexcited triplets of porphyrins.[a]

Compound[b]	Solvent[c]	T/K	D/mT	E/mT	E_{av}/mT
1	5CB	110	32.6	9.7	2.1
1	toluene	120	31.7		0
2	5CB	110	32.3	9.5	
2	toluene	110	32.9	9.9	2.8
3	toluene	100	32.9		0
3	5CB	110	32.6	10.0	
4	5CB	110	33.9	4.3	
4	toluene	120	34.3	3.2	
5	5CB	110	31.8		
5	Triton X	110	31.4		
5	MTHF/toluene	110	31.6		
6-H_2	5CB	120	32.4	9.7	
6-H_2	toluene	100	33.0	10.1	
7	5CB	160	33.0		0
7	toluene	100	32.9		0
7-H_2	5CB	110	32.5		0
7-H_2	toluene	100	32.9		0
8	5CB	160	33.0		0
8	toluene	100	33.0		0
9-H_2	toluene	100	32.6		
10-H_2	toluene	100	32.7		
11	MTHF/toluene	100	32.7		0
11	Triton X	110	32.6		0
11-H_2	Triton X	110	32.6		0
12	MTHF/toluene	100	32.6		0
12	Triton X	120	32.6		0
12-H_2	MTHF/toluene	100	32.5		0
12-H_2	toluene	100	31.6		0
13	toluene	100	34.9	3.8	
13	5CB	100	34.9	3.7	
14	toluene	100	35.0	4.5	
14	5CB	100	35.2	3.7	
15	toluene	100	37.4		0

[a] Estimated errors: ±0.2 mT. [b] Hydroquinones are denoted by appending -H_2 to the compound number of the respective quinone. [c] MTHF/toluene denotes a mixture of 30% MTHF and 70% toluene (v/v); Triton X stands for Triton X-100 reversed micelles; and 5CB is the liquid crystal 4-cyano-4'-pentylbiphenyl.

an exception, making them suitable triplet spin probes for studying alignment effects.

Acknowledgements

Most of the compounds were prepared by Dr Jörg von Gersdorff, Hans Möβler, Hans Newman and Dr Licheng Sun, who are gratefully acknowledged. We thank the Deutsche Forschungsgemeinschaft (SFB project 337 and normal funding), the Fonds der Chemischen Industrie and the Volkswagen-Stiftung for financial support.

References

1 M. Bixon, J. Fajer, G. Feher, J. H. Freed, D. Gamliel, A. J. Hoff, H. Levanon, K. Möbius, R. Nechushtai, J. R. Norris, A. Scherz, J. L. Sessler and D. Stehlick, *Isr. J. Chem.*, 1992, **32**, 363, and references therein.
2 K. Hasharoni, H. Levanon, J. von Gersdorff, H. Kurreck and K. Möbius, *J. Chem. Phys.*, 1993, **98**, 2916.
3 L. Sun, J. von Gersdorff, D. Niethammer, P. Tian and H. Kurreck, *Angew. Chem.*, 1994, **106**, 2396; *Angew. Chem., Int. Ed. Engl.*, 1994, **33**, 2318.
4 V. Grebel and H. Levanon, *Chem. Phys. Lett.*, 1980, **72**, 218.
5 O. Gonen and H. Levanon, *J. Phys. Chem.*, 1985, **89**, 1637.
6 S. Michaeli, M. Hugerat, H. Levanon, M. Bernitz, A. Natt and R. Neumann, *J. Am. Chem. Soc.*, 1992, **114**, 3612.
7 J. von Gersdorff, B. Kirste and H. Kurreck, *Liebigs Ann. Chem.*, 1993, 897.
8 L. Sun, J. von Gersdorff, J. Sobek and H. Kurreck, *Tetrahedron*, 1995, **51**, 3535.
9 B. Kirste, *J. Magn. Reson.*, 1987, **73**, 213.
10 P. G. James and G. R. Luckhurst, *Mol. Phys.*, 1970, **19**, 489.
11 G. R. Luckhurst, *Mol. Cryst. Liq. Cryst.*, 1973, **21**, 125.
12 M. S. de Groot and J. H. van der Waals, *Mol. Phys.*, 1960, **3**, 190.
13 J. Fajer and M. S. Davis, in *The Porphyrins*, ed. D. Dolphin, Academic Press, New York, 1979, vol. 4, ch. 4, p. 218.
14 C. Blättler and H. Paul, *Res. Chem. Intermed.*, 1991, **16**, 201.
15 A. J. Hoff, in *Proceedings of the International Workshop on Electron Magnetic Resonance of Disordered Systems*, ed. N. D. Yordanov, World Scientific, Singapore, 1991, pp. 192–229 (see p. 220).
16 P. J. Hore, D. J. Riley, J. J. Semlyen, G. Zwanenburg and A. J. Hoff, *Biochim Biophys. Acta*, 1993, **1141**, 221.
17 J. H. van der Waals, W. G. van Dorp and T. J. Schaafsma, in *The Porphyrins*, ed. D. Dolphin, Academic Press, New York, 1979, vol. 4, ch.5, pp. 257–312.
18 A. Scherz and H. Levanon, *J. Phys. Chem.*, 1980, **84**, 324.
19 R. Breslow, H. W. Chang, R. Hill and E. Wasserman, *J. Am. Chem. Soc.*, 1967, **89**, 1112.
20 G. R. Luckhurst, G. F. Pedulli and M. Tiecco, *J. Chem. Soc. B*, 1971, 329.
21 N. Azuma, H. Ohya-Nishiguchi, J. Yamauchi, K. Mukai and Y. Deguchi, *Bull. Chem. Soc. Jpn.*, 1974, **47**, 2369.
22 N. M. Atherton, *Electron Spin Resonance*, Ellis Horwood, Chichester, 1973, p. 171.

Paper 5/02076J
Received 31*st March* 1995
Accepted 7*th July* 1995